Am J Physiol Cell Physiol 301: C1213–C1223, 2011.
First published August 10, 2011; doi:10.1152/ajpcell.00265.2011.

Purinergic regulation of high-glucose-induced caspase-1 activation in the rat retinal Müller cell line rMC-1

Katherine E. Trueblood,[1] Susanne Mohr,[2] and George R. Dubyak[1]

[1]*Department of Physiology and Biophysics, Case Western Reserve University, Cleveland, Ohio; and* [2]*Department of Physiology, Michigan State University, East Lansing, Michigan*

Submitted 26 July 2011; accepted in final form 4 August 2011

Trueblood KE, Mohr S, Dubyak GR. Purinergic regulation of high-glucose-induced caspase-1 activation in the rat retinal Müller cell line rMC-1. *Am J Physiol Cell Physiol* 301: C1213–C1223, 2011. First published August 10, 2011; doi:10.1152/ajpcell.00265.2011.—Chronic activation of proinflammatory caspase-1 in the retinas of diabetic animals and patients in vivo and retinal Müller cells in vitro is well documented. In this study we characterized how elevated glucose and extracellular purines contribute to the activation of caspase-1 in a cultured rat Müller cell (rMC-1) model. The ability of high glucose (25 mM, 24 h) to activate caspase-1 was attenuated by either apyrase, which metabolizes extracellular ATP to AMP, or adenosine deaminase (ADA), which metabolizes extracellular adenosine to inosine. This suggested that autocrine stimulation of ATP-sensing P2 receptors and adenosine-sensing P1 receptors may in part mediate the response to high glucose. Exogenous ATP, 5′-*N*-ethylcarboxamido-adenosine (NECA), a nonselective P1 receptor agonist, or forskolin (FSK) increased caspase-1 activity in rMC-1 cells cultured in control glucose (5 mM) medium. Accumulation of active caspase-1 was also increased by dipyridamole, which suppresses adenosine reuptake. High-glucose stimulation of caspase-1 was attenuated by suramin, a nonselective P2 antagonist, or A2 adenosine receptor antagonists, but not by antagonism of P2X7 ATP-gated ion channel receptors. Although high glucose increased P2X7 mRNA, neither P2X7 protein nor function was detected in rMC-1 cells. The increased caspase-1 activity stimulated by high glucose, FSK, NECA, or ATP was correlated with increased gene expression of caspase-1 and thioredoxin-interacting-protein (TXNIP). These findings support a novel role for autocrine P1 and P2 purinergic receptors coupled to cAMP signaling cascades and transcriptional induction of caspase-1 in mediating the high-glucose-induced activation of caspase-1 and secretion of IL-1β in a cell culture model of nonhematopoietic retinal Müller cells.

sterile inflammation; hyperglycemia; inflammasome; purinergic signaling

DIABETIC RETINOPATHY, a chronic, sterile inflammatory condition, is characterized by increased levels of active caspase-1 and interleukin-1-β (IL-1β), which are strongly implicated in retinal degeneration (11, 15, 22, 31, 44). One source of active caspase-1 and IL-1β are retinal Müller cells which, as the principal glia of the retina, provide vital structural and metabolic support to retinal neurons (5, 53, 54). As such, it has been postulated that inflammatory activation, characterized by increased caspase-1/IL-1β signaling and mitochondrial stress, of Müller cells under hyperglycemic conditions contributes to the development and progression of the disease (31, 44). We and others have previously reported that inhibition of caspase-1/interleukin-1β signaling prevents degeneration of retinal capillaries in diabetes (11, 15, 22, 31, 44). Our more recent studies have demonstrated that a vicious cycle of autocrine activation of caspase-1 by IL-1β is responsible for late-stage Müller cell dysfunction and retinal capillary degeneration following the initial hyperglycemic insult (K. E. Trueblood, G. R. Dubyak, S. Mohr; unpublished data). However, the exact mechanism(s) by which hyperglycemia initiates the beginning stages of chronic caspase-1 activation in Müller cells was not elucidated.

Caspase-1 activation has been best described in monocyte/macrophage-lineage leukocytes, which are the predominant sources of IL-1β in most inflamed tissues. Accumulation of active caspase-1 in these cells is mediated by the assembly of "inflammasome" platforms that recruit the zymogen form of caspase-1 (procaspase-1) to signaling complexes based on adapter proteins belonging to the NLR [nucleotide-binding domain (NBD) and leucine-rich repeat (LRR) containing] family (39). Although most NLR proteins are targeted by various pathogen-associated molecular pattern (PAMP) ligands (e.g., bacterial flagellin or DNA/RNA fragments) that accumulate during microbial infection, NLRP3 (NBD-, LRR-, and PYR-containing protein 3, also known as cyropyrin) is targeted by multiple danger-associated molecular pattern (DAMP) ligands [such as ATP or monosodium urate (MSU) crystals] that are released from dead or damaged mammalian cells within tissue sites of sterile injury and inflammation (7, 37). Recent studies have described NLRP3 inflammasomes as a distinct mechanism of caspase-1 activation in multiple inflammatory diseases with links to metabolic dysregulation (23, 28, 42, 43). Notably, purinergic signaling involving autocrine or paracrine activation of ionotropic P2X7 receptors has garnered much attention with regard to its role in the activation of NLRP3/caspase-1 signaling in hematopoietic cells such as macrophages (4, 13, 21, 27). However, NLRP3 inflammasomes also mediate caspase-1 activation in nonhematopoietic cell types such as pancreatic β-islet cells and adipocytes (23, 59).

The expression of P2X7R and other purinergic receptors has been described in Müller cells from some, but not all, species and in other retinal cell types with proposed roles in osmotic regulation or metabolism of retinal neurotransmitters (32, 51). Given the established role of P2X7R in driving NLRP3/caspase-1 activation in hematopoietic cells and the reported ability of hyperglycemia to upregulate NLRP3/caspase-1 signaling in nonhematopoietic cells, we designed experiments to characterize the potential contribution of purinergic signaling to high-glucose-induced caspase-1 activation in the rat retinal Müller cell line (rMC-1). Although upregulation of P2X7R expression and function occurs in various diabetic tissues, it was important to consider whether metabolic stress induction

Address for reprint requests and other correspondence: G. R. Dubyak Dept. of Physiology and Biophysics, School of Medicine, Case Western Reserve Univ., 10900 Euclid Ave, Cleveland, OH 44106-4970 (e-mail: gxd3@case.edu).

of caspase-1 inflammasomes may alternatively involve P2X7-independent but purine-dependent pathways (32, 41). Indeed, our findings suggest that autocrine stimulation of adenosine-sensing P1 receptors and P2 receptor subtypes other than P2X7R mediate the caspase-1 activation response of Müller cells to high glucose. Moreover, the ability of forskolin (FSK) to mimic the stimulatory effects of high glucose or purinergic agonists is consistent with a likely role for cAMP signaling in the regulation of caspase-1 in this nonhematopoietic glial cell model.

MATERIALS

Nucleotides, adenosine deaminase (ADA), apyrase (grade I), forskolin, dipyridimole (DIPYR), TRIzol, 7-amino-4-trifluoromethylcoumarin (AFC), and ethidium bromide were from Sigma (St. Louis, MO). 5′-*N*-ethylcarboxamido-adenosine (NECA), A4387079, AZ10606120, suramin, 8-cyclopentyl-1,3-dipropylxanthine (DPCPX), MRS1754, and SCH442416 were from TOCRIS (Ellisville, MO). *S*-(4-nitrobenzyl)-6-thioguanosine (NBTG) was from RBI (Natick, MA). Anti-Glut1 primary antibody was from AbCam (Cambridge, MA). Anti-VDUP-1/thioredoxin-interacting-protein (TXNIP) was from MBL (Woburn, MA). Primary antibodies against rat P2X7R (APR-004 and APR-008) were from Alamone Labs (Jerusalem, Israel). Goat anti-rabbit IgG conjugated to horseradish peroxidase (HRP) was from Santa Cruz Biotechnology (Santa Cruz, CA). Goat anti-rabbit IgG conjugated to FITC and fura2-AM were from Invitrogen (Carlsbad, CA). The fluorogenic caspase-1 substrate VI (Z-YVAD-AFC) was from Calbiochem/EMD (San Diego, CA). Bradford protein assay reagent was from Bio-Rad (Hercules, CA). Sulfo-NHS-biotin and enhanced chemiluminescence (ECL) detection reagent was from Pierce (Rockford, IL). RT^2 SYBR Green/ROX qPCR Master Mix (PA-012) and predesigned qPCR primers for rat P2X7R (PPR44893A), rat P2Y2R (PPR45235B), rat TXNIP (PPR42837A), rat caspase-1 (PPR06427A), rat GAPDH (PPR06557A), and rat 18S ribosomal RNA (PPR57734E) were from SA Biosciences (Frederick, MD). RNeasy Mini Kits were from Qiagen (Valencia, CA). Transcriptor first-strand cDNA synthesis kit was from Roche (Indianapolis, IN).

Methods

Tissue culture. The rMC-1 line (obtained from Dr. V. R. Sarthy, Northwestern University, IL) was utilized in these studies. rMC-1 cells in 10-cm dishes were grown in 5 mM glucose-DMEM supplemented 10% FBS and 1% penicillin-streptomycin (P/S) at 37°C and 5% CO_2 in a humidified incubator. All experiments were performed using cells at passages <37.

HEK293 cells stably transfected with the wild-type rat P2X7R (HEK-rP2X7 cells) were selected for, and maintained in, DMEM (25 mM glucose, 10% CS, 1% L-glutamine, 1% P/S) supplemented with 400 μg/ml G418 at 37°C and 5% CO_2 in a humidified incubator. Expression of rP2X7R was verified using Western blot and FACS analysis.

High-glucose treatment. rMC-1 cells(1×10^6) were transferred from their standard growth medium to either normal/control (5 mM) glucose DMEM or high (25 mM) glucose DMEM supplemented with 2% FBS and 1% P/S for 24 h before experimental assays. Cells treated with normal glucose DMEM supplemented with 2% FBS served as controls.

Treatment with exogenous nucleotides or NECA. rMC-1 cells(1×10^6/10 cm dish) were transferred to either normal glucose or high-glucose DMEM with 2% FBS and 1% P/S. The DMEM was then supplemented as indicated in particular experiments with various nucleotides (ATP, ADP, or UTP at 10 μM-10 mM final concentration) or the adenosine analog NECA (at 10–100 μM final concentration), and treated cells were incubated for 24 h before experimental assays.

Treatment with nucleotide/nucleoside scavenging enzymes, P1/P2 receptor antagonists, or nucleoside transport inhibitors. rMC-1 cells (1×10^6/ 10 cm plate) were transferred to either normal or high-glucose DMEM supplemented with 2% FBS and 1% P/S and then incubated in the presence or absence of either apyrase (5 U/ml), ADA (2 U/ml), suramin (10 μM), A438079 (10–20 μM), AZ 10606120 (10 μM), MRS1754 (10 μM), SCH442416 (10 μM), DPCPX (10 μM), NBTG (80 μM), or DIPYR (5 μM) for 24 h before experimental analysis.

Whole cell lysate preparation. After the 24-h incubations/treatments in normal or high-glucose DMEM described above, rMC-1 cells (1×10^6) were lysed in 200 μl of 3-[(3-cholamidopropyl)dimethylammonio]-1-propanesulfonate (CHAPS) lysate buffer [100 mM HEPES, pH 7.5, 10% sucrose, 0.1% CHAPS, 1 mmol/l EDTA, 1 mM PMSF, and leupeptin (10 μg/ml)] and then processed exactly as described previously (30, 31, 44, 53, 54). Supernatants were retained, assayed for protein content by the Bradford method, and then used for caspase-1 activity measurements.

Membrane protein extraction and preparation. After treatment, rMC-1 and HEK-rP2X7R cells were washed with ice-cold PBS, permeabilized with 20 μl of digitonin (5 mg/ml) for 5 min at 37°C to release soluble cytosolic proteins, and washed again with ice-cold PBS. The permeabilized cells were lysed with 150 μl of radioimmunoprecipitation assay extraction buffer (RIPA) [1% Nonidet P-40, 0.5% Na-deoxycholate, 0.1% SDS (pH 7.4) in PBS] containing PMSF, leupeptin, and aprotinin for 15 min on ice. Lysates were centrifuged at 10,000 *g* for 10 min at 4°C. Supernatants were retained, assayed for protein content by the Bradford method, and then prepared for SDS-PAGE.

Caspase-1 activity assays. Caspase-1 activities were measured as described previously (25, 26, 44, 47, 52). Briefly, the caspase-1-specific substrate (YVAD-AFC; 2.5 μmol/l) was incubated with equal amounts of sample (15 μg) for 1 h at 32°C. Fluorescence was detected by a Tecan Spectra FluorPlus fluorescence plate reader (excitation: 400 nm, emission: 510 nm). Caspase activity was calculated against an AFC standard curve (data expressed as pmol·AFC^{-1}·mg protein^{-1}·min^{-1}).

Western blot analysis. Samples (20 μg) were separated by 15% SDS-PAGE gels and transferred onto polyvinylidene fluoride. Membranes were blocked in 4% nonfat dry milk and incubated with primary anti-rP2X7R (APR-004, 0.3 μg/ml or APR-008, 0.9 μg/ml), anti-GLUT1 (1 μg/ml), anti-TXNIP (1 μg/ml), or anti-β actin (1:10,000) overnight at 4°C. Incubation with secondary HRP-conjugated antibodies (1:3,000) was completed for 1 h at room temperature. Membranes were developed using enhanced chemiluminescence detection reagent.

Measurement of nucleotide-induced Ca^{2+} mobilization. HEK-rP2X7R or rMC-1 were trypsinized to generate cell suspensions (10^6/ml) and then incubated with 1 μM fura2-AM for 30–60 min. Cytosolic [Ca^{2+}] in the fura2-loaded cell suspensions before and after stimulation with ATP, ADP, or UTP (1 μM-1 mM) was measured and calibrated using a fluorimeter as previously described (18). Because rMC-1 and HEK293 cells express Gq-coupled, Ca^{2+}-mobilizing P2Y2 receptors, analysis of possible P2X7R-mediated Ca^{2+} influx was assayed by first treating the cells with 30 μM UTP to activate and desensitize the P2Y2 receptors before stimulation of P2X7 by the indicated concentrations of ATP.

Measurement of ATP-stimulated K^+ efflux by atomic absorbance spectrophotometry. rMC-1 or HEK293-rP2X7 cells were plated in 12-well dishes and incubated in either normal or high-glucose DMEM for 24 h. The cell monolayers were washed once with PBS and then bathed in 1 ml of a basal salt solution (130 mM NaCl, 5 mM KCl, 1 mM $MgCl_2$, 1.5 mM $CaCl_2$, 25 mM NaHEPES, pH 7.5, 5 mM glucose, 0.1% bovine serum albumin) for 5 min at 37°C. Cells were then stimulated without or with ATP (1–5 mM) for 10 min at 37°C. ATP-containing medium was rapidly aspirated to terminate K^+ efflux reactions and replaced with 1 ml of 10% nitric acid at room temper-

ature for 3–4 h to extract K^+ from the cell monolayers. K^+ content was quantified using atomic absorbance spectroscopy (20).

Quatitative PCR analysis of mRNA transcripts encoding rP2X7R, rP2Y2R, TXNIP, and caspase-1. Total RNA was extracted by TRIZol reagent from rMC-1 cells incubated for 24 h in normal or high-glucose DMEM as described previously (36). A Transcriptor First Strand cDNA Synthesis kit was utilized for synthesis of first-strand cDNA from purified RNA. Quantitative PCR (qPCR) analysis of P2X7R, P2Y2R, TXNIP, caspase-1, GAPDH, or 18S ribosomal RNA was performed using a StepOne-Plus Real-Time PCR System (Applied Biosystems). Reactions were performed in 25-μl reaction volumes containing RT^2 SYBR Green/ROX qPCR Master Mix (12.5 μl), 1:100 dilutions of RT product, and 1 μM PCR primer pair stock and run in triplicate. Amplification cycle conditions were 95°C for 10 min followed by 40 cycles of 95°C, 15 s; 55°C, 30–40 s; and 72°C, 30 s. Melt curves were performed at the end of the reaction with all products demonstrating one predominant peak. Relative expression was calculated using the $\Delta\Delta C_t$ method using StepOne software version 2.1 with values normalized to the reference genes GAPDH or 18S rRNA.

Data Processing and Statistical Analysis

For caspase-1 experiments, the fold change in caspase-1 activity was calculated by normalizing caspase-1 activity in treated samples (high glucose and a variety of agonists/antagonists) to the paired controls (normal glucose-treated samples) for each experiment and graphed as means ± SE. For qPCR experiments, $\Delta\Delta C_t$ values were calculated compared with normal glucose controls and graphed as means ± SE. In atomic absorbance spectrophotometry experiments, intracellular K^+ concentrations were calculated compared with a K^+ standard curve, and data were expressed as means ± SE. Statistical significance was determined by ANOVA one-way analysis by comparing values in treated groups to paired normal glucose control values (correlated samples, $P < 0.05$). For details in statistical analysis see VasserStats Statistical Computation Web Site.

RESULTS

Treatment of rMC-1 Cells With Extracellular Apyrase or Adenosine Deaminase Suppresses High-Glucose-Induced Caspase-1 Activation

Purinergic regulation of caspase-1 activation in myeloid hematopoietic cells has been well documented (21, 27). To determine whether extracellular purines are involved in high-glucose-induced caspase-1 activation in nonhematopoietic Müller glial cells, we cultured the rMC-1 line in high-glucose medium supplemented with potato apyrase, which is a broad-spectrum ATP scavenger that serially metabolizes ATP to ADP and then AMP. Apyrase treatment significantly reduced high-glucose-induced caspase-1 activation (Fig. 1*A*). In addition to ATP, extracellular adenosine can regulate pro-inflammatory processes (19). Scavenging of endogenous extracellular adenosine by treatment with ADA, which rapidly converts adenosine to inosine, also significantly reduced high-glucose-induced caspase-1 activation (Fig. 1*B*). The ability of ATP- and adenosine-scavenging enzymes to suppress high-glucose-induced caspase-1 activation suggested that autocrine stimulation of both adenosine-sensing P1 receptors and ATP-sensing P2 receptors may cooperatively mediate this response of rMC-1 cells to elevated glucose.

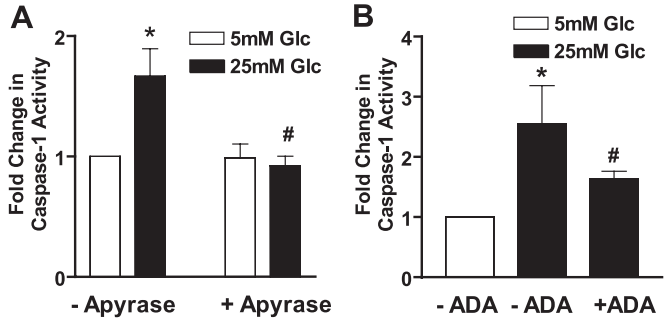

Fig. 1. Treatment of retinal Müller cells (rMC-1) with extracellular apyrase or adenosine deaminase (ADA) suppresses high-glucose-induced caspase-1 activation rMC-1 cells were incubated in control (5 mM) or high (25 mM) glucose (Glc) medium ± apyrase (5 U/ml) (*A*) or ± ADA (2 U/ml) (*B*). Caspase-1 activity was measured (as described in METHODS) after 24 h, normalized to the control activity, and expressed as means ± SE ($n = 5$). *$P < 0.02$ compared with control, #$P < 0.004$ compared with high glucose (ANOVA).

Treatment of rMC-1 Cells With Exogenous ATP, Exogenous Adenosine Analog, or Adenosine Uptake Inhibitors Mimics High-Glucose-Induced Caspase-1 Activation

Because apyrase reduced high-glucose-induced caspase-1 activation, we tested whether exogenous ATP (the primary agonist for P2X7R and other P2XR and P2YR subtypes) might directly induce caspase-1 activation in retinal Müller cells incubated under normal glucose conditions. The caspase-1 activation response of rMC-1 cells treated with 5 mM ATP in normal glucose medium was similar in magnitude to that induced by high-glucose medium in the absence of exogenous ATP (Fig. 2*A*); inclusion of 5 mM ATP in the high-glucose medium did not produce an additive or synergistic effect. Caspase-1 activation was increased by extracellular ATP in a concentration-dependent manner under normal glucose conditions (Fig. 2*B*) but required supramillimolar ATP. This may reflect a requirement for sustained elevation of extracellular ATP (averaged over the 24-h test period) in the 10–100 μM concentration range that facilitates maximal activation of most P2 receptor subtypes (9, 45). Indeed, a 5 mM pulse of exogenous ATP was rapidly (90% clearance within 6 h) metabolized by robust ecto-ATPase activities associated with both the rMC-1 cell surface and the 2% FBS component of the DMEM; rMC-1 cultured in normal or high-glucose medium exhibited similar rates of exogenous ATP clearance (data not shown).

A requirement for supramillimolar ATP could also indicate a role for sustained accumulation of extracellular ADP, which is the preferred agonist for the P2Y1, P2Y12, and P2Y13 receptor subtypes (45). However, inclusion of 5 mM ADP in the normal glucose DMEM did not significantly increase caspase-1 activity (Fig. 2*A*). Moreover, co-incubation with both high glucose and 5 mM exogenous ADP partially attenuated the caspase-1 activation to high glucose alone. Supramillimolar ATP could also drive the ecto-nucleotide diphosphokinase-mediated transphosphorylation of released UDP to generate extracellular UTP, a potent agonist for the P2Y2 and P2Y4 receptor subtypes. Like ADP but unlike ATP, 5 mM UTP alone did not increase caspase-1 activation in rMC-1 cells incubated in

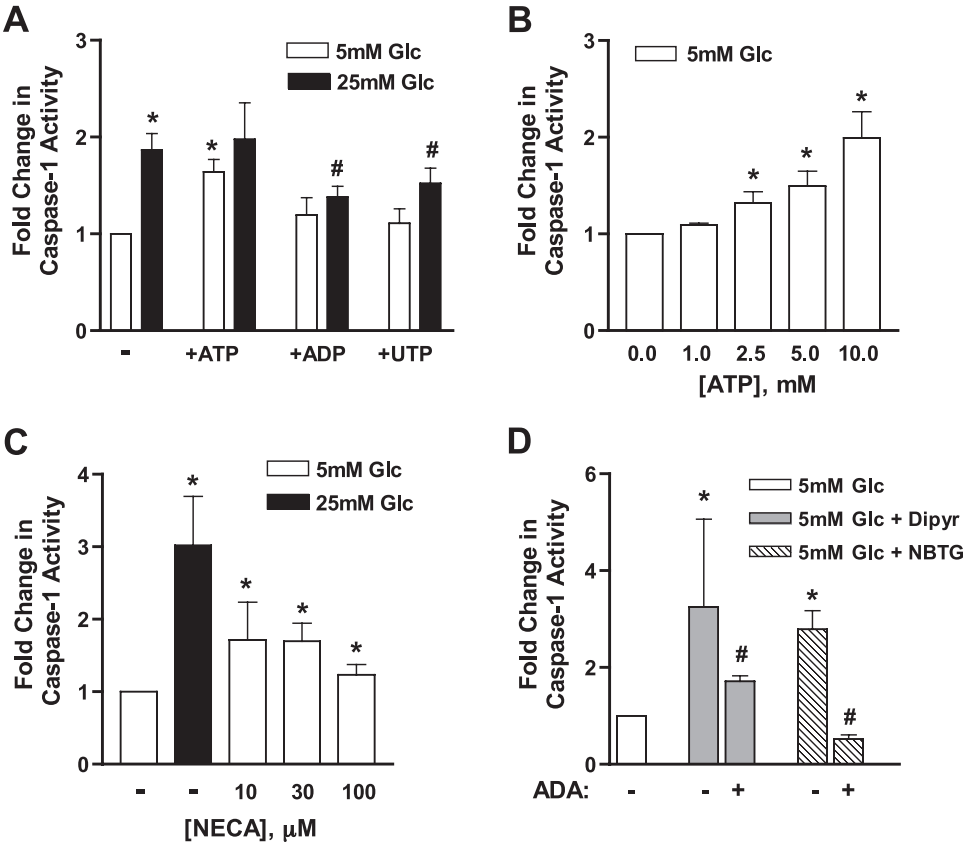

Fig. 2. Treatment of rMC-1 cells with exogenous ATP, exogenous adenosine analog, or adenosine uptake inhibitors mimics high-glucose-induced caspase-1 activation. *A*: rMC-1 cells were incubated in control or high-glucose medium ± ATP (5 mM), ADP (5 mM), or UTP (5 mM). Caspase-1 activity was measured after 24 h, normalized to the control activity, and expressed as means ± SE ($n = 5$). *$P < 0.0002$ compared with control, #$P < 0.05$ compared with + high-glucose samples (ANOVA). *B*: rMC-1 cells were incubated in control (5 mM Glc) medium supplemented with the indicated concentrations of ATP (1–10 mM). Caspase-1 activity was measured after 24 h, normalized to the control activity, and expressed as means ± SE ($n = 5$). *$P < 0.0002$ compared with control (ANOVA). *C*: rMC-1 cells were incubated in control medium, high-glucose medium, or control medium + 5′-*N*-ethylcarboxamido-adenosine (NECA; 10, 30, 100 μM). Caspase-1 activity was measured after 24 h, normalized to the control activity, and expressed as means ± SE ($n = 5$). *$P < 0.03$ compared with control (ANOVA). *D*: rMC-1 cells were incubated in control (5 mM glucose) medium supplemented with 80 μM dipyridamole (Dipyr) or 5 μM *S*-(4-nitrobenzyl)-6-thioguanosine (NBTG), with and without ADA (2 U/ml). Caspase-1 activity was measured after 24 h, normalized to the control activity, and expressed as means ± SE; $n = 5$. *$P < 0.05$ compared with control. #$P < 0.05$ compared with +Dipyr or +NBTG alone (ANOVA).

control glucose medium but did attenuate the increase in caspase-1 elicited under high-glucose conditions (Fig. 2*A*).

Given that ADA attenuated high-glucose-induced caspase-1 activation (Fig. 1*B*), we tested whether exogenous adenosine also stimulates caspase-1 under control glucose conditions. Because extracellular adenosine per se can be rapidly cleared by endogenously expressed ADA or nucleoside transporters, rMC-1 cells were treated with varying concentrations (10–100 μM) of NECA, a stable adenosine analog and nonselective agonist for all four adenosine receptor subtypes (16). At 10 or 30 μM, NECA significantly increased caspase-1 activity compared with normal glucose controls but not to the magnitude observed with high-glucose treatment (Fig. 2*C*). Notably, the efficacy of NECA did not increase, but modestly decreased, as the test concentration was elevated to 100 μM.

To determine whether increased levels of endogenously produced extracellular adenosine also stimulate caspase-1 activity, we treated rMC-1 cells with DIPYR or NBTG, which inhibit the nucleoside transporters that can facilitate reuptake of extracellular adenosine (16). Both reagents stimulated caspase-1 activation in normal glucose-treated rMC-1, and this effect was attenuated when the cells were treated with either reagent in combination with ADA (Fig. 2*D*).

Treatment of rMC-1 Cells With Suramin or Adenosine Receptor Antagonists Suppresses High-Glucose-Induced Caspase-1 Activation

Given the stimulatory effects of exogenous ATP, NECA, and the adenosine reuptake inhibitors, we hypothesized that antagonism of either P2 nucleotide receptors or P1 adenosine receptors would reduce high-glucose-induced caspase-1 activation. The nonselective P2 receptor inhibitor suramin, which targets the widely expressed P2Y2 receptor and other P2 subtypes (9, 45), reduced high-glucose-induced caspase-1 activation and also basal caspase-1 activity (Fig. 3*A*). DPCPX, which acts as a nonselective adenosine receptor antagonist at high (>1 μM) concentrations (16), also markedly reduced high-glucose caspase-1 activation (Fig. 3*B*). The effect of 10 μM DPCPX was mimicked by the A2B antagonist MRS1754 (also at 10 μM). The A2A selective antagonist SCH442416 (at 10 μM) also significantly reduced high-glucose-induced caspase-1 activation but with reduced efficacy relative to DPCPX or MRS1754.

No Significant Role For P2X7 Receptors in Purinergic Regulation of High-Glucose-Induced Caspase-1 Activation

Supramillimolar concentrations of extracellular ATP were required for activation of caspase-1 in rMC-1 cells under normal glucose conditions (Fig. 2*B*). P2X7R is the P2 subtype with lowest ATP affinity and is also the purinergic receptor unequivocally linked to regulation of caspase-1 activation in hematopoietic cells (12, 13). Thus we characterized P2X7R expression and its possible contribution to high-glucose-induced caspase-1 activation in rMC-1 cells using two selective P2X7R antagonists (9). Although treatment with the P2X7R-selective antagonist A438079 significantly reduced high-glucose-induced caspase-1 activation, a structurally distinct selective P2X7R antagonist AZ10606120 had no effect (Fig. 3*C*). This suggested that the ability of A438079 to attenuate

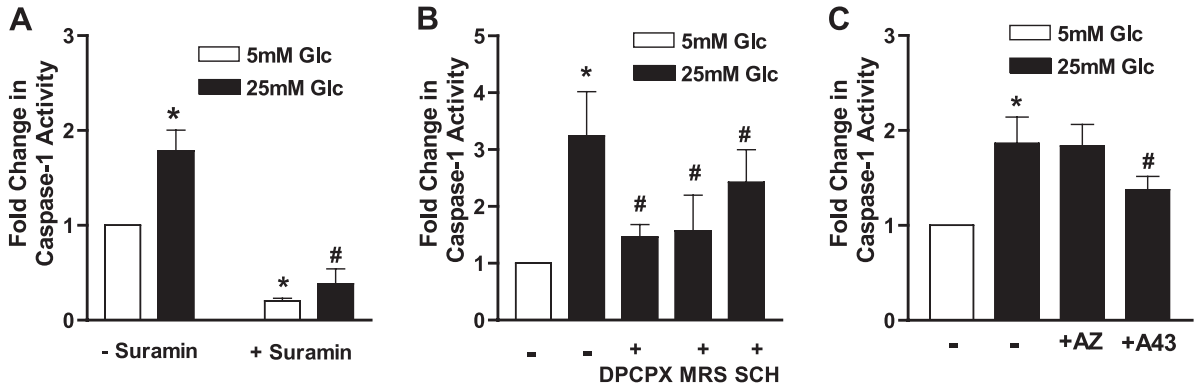

Fig. 3. Treatment of rMC-1 cells with suramin or adenosine receptor antagonists, but not P2X7 antagonists, suppresses high-glucose-induced caspase-1 activation. *A*: rMC-1 cells were incubated in control medium ± suramin (10 μM) or high-glucose medium ± suramin (10 μM). Caspase-1 activity was measured after 24 h, normalized to the control activity, and expressed as means ± SE; $n = 5$. *$P < 0.02$ compared with controls, #$P < 0.004$ compared with high glucose (ANOVA). *B*: rMC-1 cells were incubated in control medium or in high-glucose medium ± 8-cyclopentyl-1,3-dipropylxanthine (DPCPX; 10 μM), MRS1754 (10 μM), or SCH442416 (10 μM). Caspase-1 activity was measured after 24 h, normalized to the control activity, expressed as means ± SE. *$P < 0.004$ compared with 5 mM Glc, #$P < 0.05$ compared with 25 mM Glc; $n = 5$. *C*: rMC-1 cells were incubated in control medium or in high-glucose medium ± A438079 (10 μM) ($n = 8$) or AZ10606120 (10 μM) ($n = 5$). Caspase-1 activity was measured after 24 h, normalized to the control activity, and expressed as means ± SE. *$P < 0.0001$ compared with control, #$P < 0.02$ compared with high glucose (ANOVA).

caspase-1 activation may reflect an off-target effect rather than specific antagonism of P2X7R.

We performed qPCR analysis for P2X7R, P2Y2R, and TXNIP mRNA expression in normal and high-glucose-treated cells. TXNIP was assayed as a positive control gene with a known glucose-responsive promoter and because of its link to hyperglycemia-induced mitochondrial dysfunction and caspase-1 activation (2, 17, 23, 33, 59). Figure 4*A* shows that high glucose elicited severalfold increases in TXNIP and P2X7R transcript levels. Western blot analysis of whole cell lysates indicated that the increased TXNIP mRNA levels were matched by increased TXNIP protein expression confirming the glucose responsiveness of rMC-1 cells (Fig. 4*B*, *bottom right*). In contrast, Western blot analysis of either whole cell lysates (not shown) or membrane-enriched extracts from digitonin-treated samples (Fig. 4*B*, *left*) failed to reveal measurable levels of P2X7R protein in control or high-glucose-treated rMC-1 cells. These analyses used two different P2X7R antibodies: one that recognizes intracellular COOH-terminal residues from the full-length 595-amino acid rat P2X7R and another raised against an amino acid sequence from the extracellular loop of P2X7R (Fig. 4*B*, *top right*). The latter antibody can recognize both full-length P2X7R and recently identified P2X7R splice variants with truncated intracellular COOH-termini (1). Positive and negative control samples verified that both antibodies detected a 78-kDa band in extracts from HEK293 cells stably transfected with rat P2X7R cDNA (HEK-P2X7) but not from wild-type HEK293 cells. Membrane extracts from both control and high-glucose-treated rMC-1 cells were positive for the Glut1 glucose transporter, an intrinsic membrane protein expressed by Müller cells (Fig. 4*B*). To enrich for possible low abundance cell surface P2X7R proteins, control or high-glucose-treated cells were incubated with a membrane-impermeant biotinylating crosslinker before detergent extraction and precipitation with streptavidin-agarose beads. However, anti-P2X7 Western blots of the streptavidin precipitates again failed to detect immunoreactive protein in the rMC-1 samples (data not shown).

As a well-characterized functional readout of expressed P2X7R, we compared the ability of supramillimolar ATP to induce K^+ efflux from the rMC-1 cells versus HEK-P2X7 cells (20). Whereas HEK-rP2X7R cells released >50% of their intracellular K^+ pool during a 10-min stimulation with 5 mM ATP, no significant decreases in intracellular K^+ were observed in either control or high-glucose-treated rMC-1 cells challenged with 5 mM ATP (Fig. 4*C*). As an additional index of P2X7R function, we assayed ATP-triggered induction of nonselective pores permeable to organic molecules up to 900 Da in mass (12, 13, 18). No ATP-induced accumulation of fluorescent ethidium-DNA complexes, indicative of increased influx of the otherwise size-excluded ethidium$^+$ dye (M_r 390 Da), was observed in control or high-glucose-treated rMC-1 cells (data not shown).

Activation of Caspase-1 By High-Glucose, NECA, or ATP is Mimicked by Forskolin and Correlated With Increased Gene Expression of Caspase-1 and TXNIP

The antagonistic effects of MRS1754 and SCH442416 (Fig. 3*B*) indicated that the adenosinergic component of high-glucose-induced caspase-1 activation may reflect agonistic input from A2 receptor subtypes coupled to Gs/adenylyl cyclase/cAMP signaling (16). Notably, treatment of rMC-1 cells with FSK, a direct activator of adenylyl cyclase, mimicked the ability of high-glucose treatment or NECA to increase caspase-1 activation (Fig. 5*A*). Almeida et al. (3) recently reported that treatment of osteoblasts with FSK or Gs-coupled prostaglandin E receptor agonists increased caspase-1 activity secondary to the cAMP-dependent stimulation of caspase-1 gene expression. We observed that FSK similarly induced a marked upregulation of caspase-1 expression in rMC-1 cells (Fig. 5*B*). Caspase-1 mRNA transcripts were also elevated in cells treated with high glucose, NECA (30 μM), or ATP (5 mM) but not to the magnitude induced by FSK. Treatment with FSK, NECA, or

ATP also induced accumulation of TXNIP mRNA but to levels lower than in high-glucose-stimulated cells (Fig. 5*B*).

rMC-1 Cells Express Gq-Coupled, Ca^{2+}-Mobilizing P2Y2/P2Y4 and P2Y1 Receptors and High-Glucose Treatment Increases the Efficacy of Ca^{2+} Mobilization

The antagonistic action of suramin (Fig. 3*A*) suggested that one or more suramin-sensitive P2Y or P2X receptor subtypes may mediate the contribution of autocrine ATP to high-glucose-induced caspase-1 activation in rMC-1 cells. A general response to activation of most P2Y and P2X receptor subtypes is marked perturbation in ion homeostasis, including rapid mobilization or influx of Ca^{2+} (9, 18, 45). Control rMC-1 cells exhibited robust and equivalent Ca^{2+} mobilization responses to 100 μM ATP or UTP, whereas 100 μM ADP was less efficacious (Fig. 6*A*). With [ATP] ≤100 μM, the ATP concentration-response relationship was characterized by an EC50 of ~3 μM and a plateau phase at 10–100 μM; increasing ATP to 1 mM produced a further increase in peak [Ca^{2+}] (Fig. 6*B*). Treatment with high glucose increased the efficacy of ATP as a Ca^{2+}-mobilizing agonist at concentrations >10 μM. The UTP concentration-response in control rMC-1 cells was similar to that of ATP but without the secondary increase in peak Ca^{2+} mobilization as UTP was increased to 1 mM (Fig. 6*C*). As for ATP, growth in high glucose potentiated the efficacy of UTP at concentrations >10 μM. The ADP concentration responses were quite different with little response at ≤10 μM and no plateau at 100 μM in cells cultured in normal or high-glucose medium (Fig. 6*D*); these results were consistent low-level expression of the ADP-selective P2Y1 subtype. Notably, initial stimulation of rMC-1 cells with UTP prevented Ca^{2+} mobilization responses to a secondary stimulation with ATP (and vice versa) indicating cross-desensitization of a common P2Y subtype that recognizes both ATP and UTP as agonists (not shown). This is consistent with both the pharmacology of the P2Y2 and/or (for this rat-derived cell type) P2Y4 subtypes (45) and the expression of P2Y2 mRNA in rMC-1 cells (Fig. 4*A*).

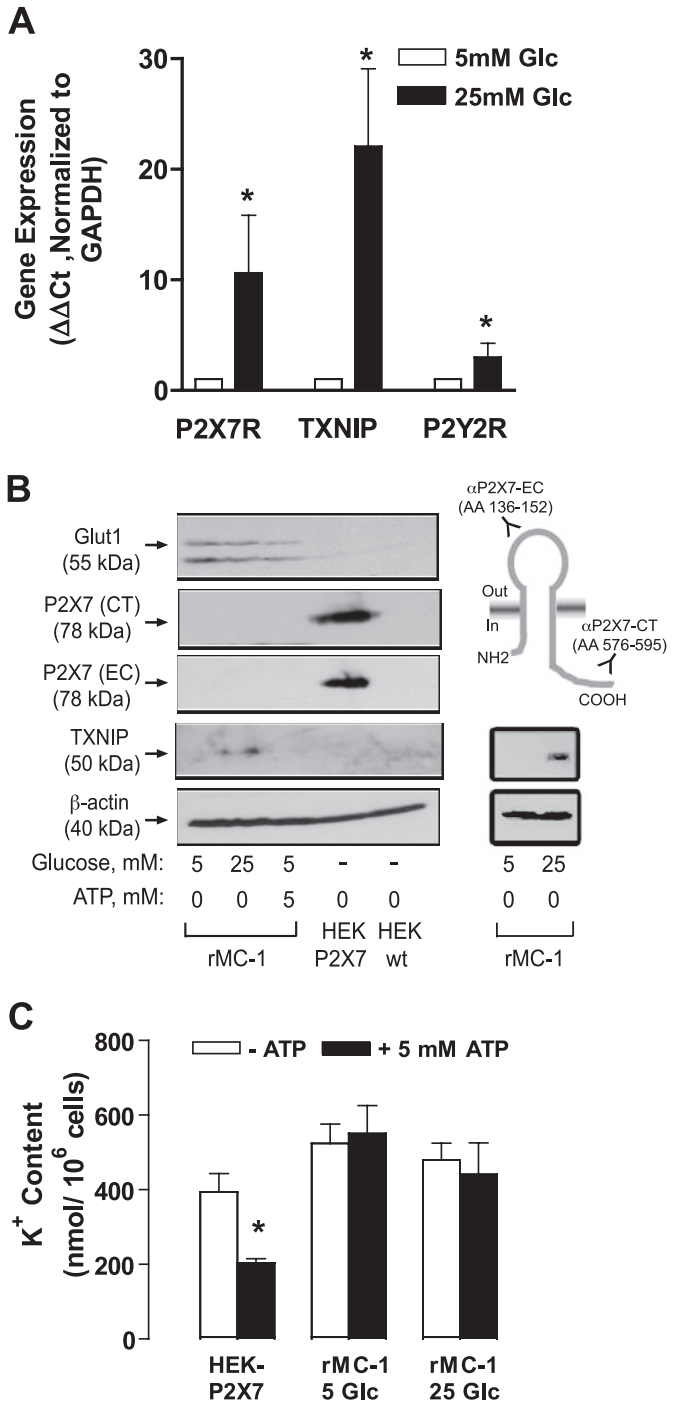

Fig. 4. rMC-1 cells do not express immunoreactive P2X7 receptor protein or functional P2X7 receptors. *A*: RNA was isolated from rMC-1 cells after incubation in control or high-glucose media for 24 h and was then reverse-transcribed to cDNA for quantitative PCR analysis of P2X7R, thioredoxin-interacting-protein (TXNIP), and P2Y2R gene expression. Target gene expression was quantified relative to the housekeeping GAPDH gene product, and the fold increases in gene expression between high glucose versus control media incubation were calculated by the $\Delta\Delta C_t$ method and graphed as means ± SE (n = 13). *$P < 0.001$ compared with control. *B*: *Left*, whole cell lysates were prepared from digitonin-treated rMC-1 cells after incubation in control medium, high-glucose medium, or control medium + 5 mM ATP for 24 h. Lysates were similarly prepared from digitonin-treated HEK-P2X7 cells or wild-type HEK293 cells. Samples were resolved by SDS-PAGE and analyzed by serial Western blots using antibodies against β-actin, TXNIP, P2X7R-COOH terminus (CT), P2X7R-extracellular loop (EC), and Glut1. Representative blots from 1 of 4 independent experiments are shown. *Right*, *top*: epitope domains of the P2X7 antibodies. *Right*, *bottom*: whole cell lysates were prepared from intact rMC-1 cells after incubation in control or high-glucose medium and for TXNIP and β-actin expression as described for left panel. *C*: rMC-1 cells in six-well plates were incubated in control or high-glucose medium for 24 h. After being washed and transfered to basal salt solution, parallel wells of adherent cells were incubated ± 5 mM ATP for 15 min before nitric acid extraction and quantification of K content by atomic absorbance spectrophotometry. HEK-P2X7 cell cultures were subjected to the identical stimulation protocol and K analysis. Data are expressed as means ± SE (n = 5). *$P < 0.002$ compared with unstimulated (0 mM ATP HEK-rP2X7R) samples (ANOVA).

DISCUSSION

Glial cell dysfunction and death have been identified as hallmarks of several neurodegenerative diseases including Alzheimer's disease, Huntington's disease, and diabetic retinopathy (5, 22, 46, 57, 60). Such diseases are also characterized by aberrant caspase-1 activation and consequent IL-1β production similar to that observed in other chronic, sterile inflammatory conditions such as arthritis and diabetes mellitus type 1 (7,

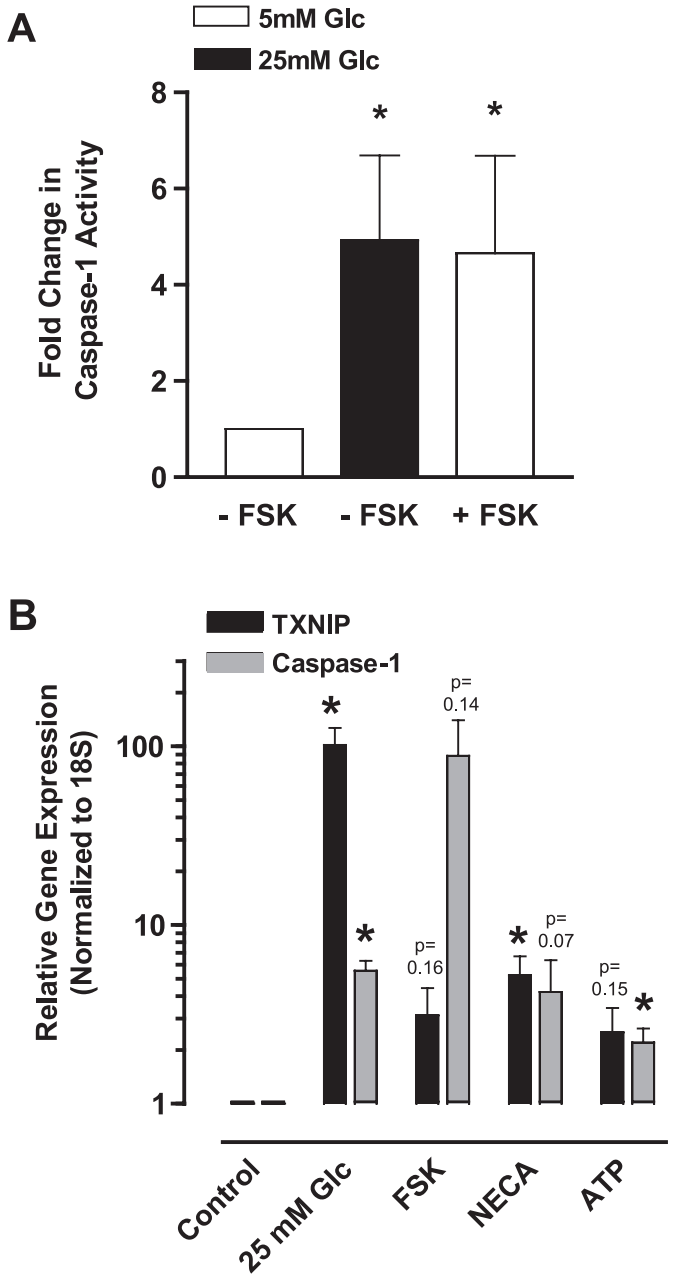

Fig. 5. Activation of caspase-1 by high glucose, NECA, or ATP is mimicked by forskolin (FSK) and correlated with increased gene expression of caspase-1 and TXNIP. *A*: rMC-1 cells were incubated in control medium ± 10 μM FSK or high-glucose medium. Caspase-1 activity was measured after 24 h, normalized to the control activity, and expressed as means ± SE ($n = 5$). *$P < 0.02$ compared with control (ANOVA). *B*: RNA was isolated from rMC-1 cells after incubation in control medium, high-glucose medium, control medium plus 10 μM FSK, control medium plus 30 μM NECA, or control medium plus 5 mM ATP for 24 h and then reverse transcribed to cDNA for quantitative PCR analysis of TXNIP and caspase-1 gene expression. Target gene expression was quantified relative to the housekeeping 18S rRNA gene product, and the fold increases in gene expression between the various treatments versus control media incubation were calculated by the $\Delta\Delta C_t$ method and graphed as means ± SE ($n = 4$). *$P < 0.05$ compared with control.

29, 35, 37). Inflammasome-based mechanisms of caspase-1 activation in myeloid hematopoietic cells in response to microbial infections or stimulation of purinergic P2X7 ATP-gated ion channel receptors have been well characterized (13, 39). Whether similar pathways underlie sterile caspase-1 activation in nonhematopoietic inflammatory cells, such as the Müller glia, which contribute to diabetic retinopathy, have not been characterized. This present study indicates that a novel purinergic signaling cascade mediates in part the ability of high-glucose stress to activate caspase-1 in the rMC-1 cell line. In contrast to the P2X7R-dependent signaling that defines purinergic regulation of caspase-1 in myeloid hematopoietic cells, this new pathway includes a key role for autocrine activation of G protein-coupled A2 adenosine receptors and cAMP-dependent signaling. Moreover, both the purinergic- and the high-glucose-stimulated components of caspase-1 regulation are correlated with increased gene expression of caspase-1 and TXNIP, an adapter protein linked to caspase-1 regulation in other nonhematopoietic cells. Finally, G protein-coupled P2Y receptors appear to drive additional signals that, depending on context, positively or negatively modulate the caspase-1 response to high glucose. Figure 7 illustrates a schematic model that encompasses the signaling pathways and network implicated by our observations.

Most cells release ATP at low rates that are counteracted by multiple ecto-nucleotidases that serially metabolize extracellular ATP into ADP, AMP, and, ultimately, adenosine for reaccumulation and regeneration of cytosolic ATP (10). Our experiments suggest that high glucose comprises a metabolic stress signal that changes the relative rates of ATP release/hydrolysis and adenosine clearance by rMC-1 cells to facilitate: *1*) steady-state concentrations of extracellular ATP, ADP, and adenosine sufficient for autocrine stimulation of various P2 nucleotide receptors and P1 adenosine receptors; and *2*) the consequent induction of P2 and P1 receptor-dependent signaling cascades that converge on activation of caspase-1. Pharmacological analyses indicated that autocrine purinergic mediation of the high-glucose-induced caspase-1 response in rMC-1 cells involves signals generated both by A2 receptors for adenosine and by apyrase- and suramin-sensitive P2 receptors for ATP. Inclusion of exogenous ATP in the control (5 mM glucose) culture medium elicited caspase-1 activation similar in magnitude to that stimulated by high glucose. Exogenous ATP will directly stimulate P2 receptors and, due to metabolism by ecto-nucleotidases, will generate adenosine for stimulation of adenosine receptors. This indicates that coactivation of P2 receptors and A2 adenosine receptors can entrain signaling pathways that lead to accumulation of active caspase-1 even in absence of high-glucose metabolic stress.

The ability of exogenous NECA to stimulate caspase-1 in the absence of high-glucose stress demonstrates that adenosine receptor signaling is sufficient for this proinflammatory response in the rMC-1 cell model, albeit at reduced efficacy in comparison to high glucose (Fig. 2*C*) or 5 mM ATP (Fig. 2*A*). Multiple reports have described the expression of functional adenosine receptors in retinal Müller cells (24, 49). Our findings represent the first linkage of these G protein-coupled receptors to caspase-1 based inflammation and support a model wherein A2 adenosine receptors, coupled to cAMP signaling, induce transcriptional upregulation of caspase-1 and TXNIP, a glucose-sensitive adapter protein linked to caspase-1 activation. All of the stimuli (high glucose, NECA, ATP, and FSK) that increased caspase-1 activity also increased caspase-1 mRNA levels in rMC-1 cells, albeit to different magnitudes (Fig. 5*B*). Myeloid hematopoietic inflammatory cells, includ-

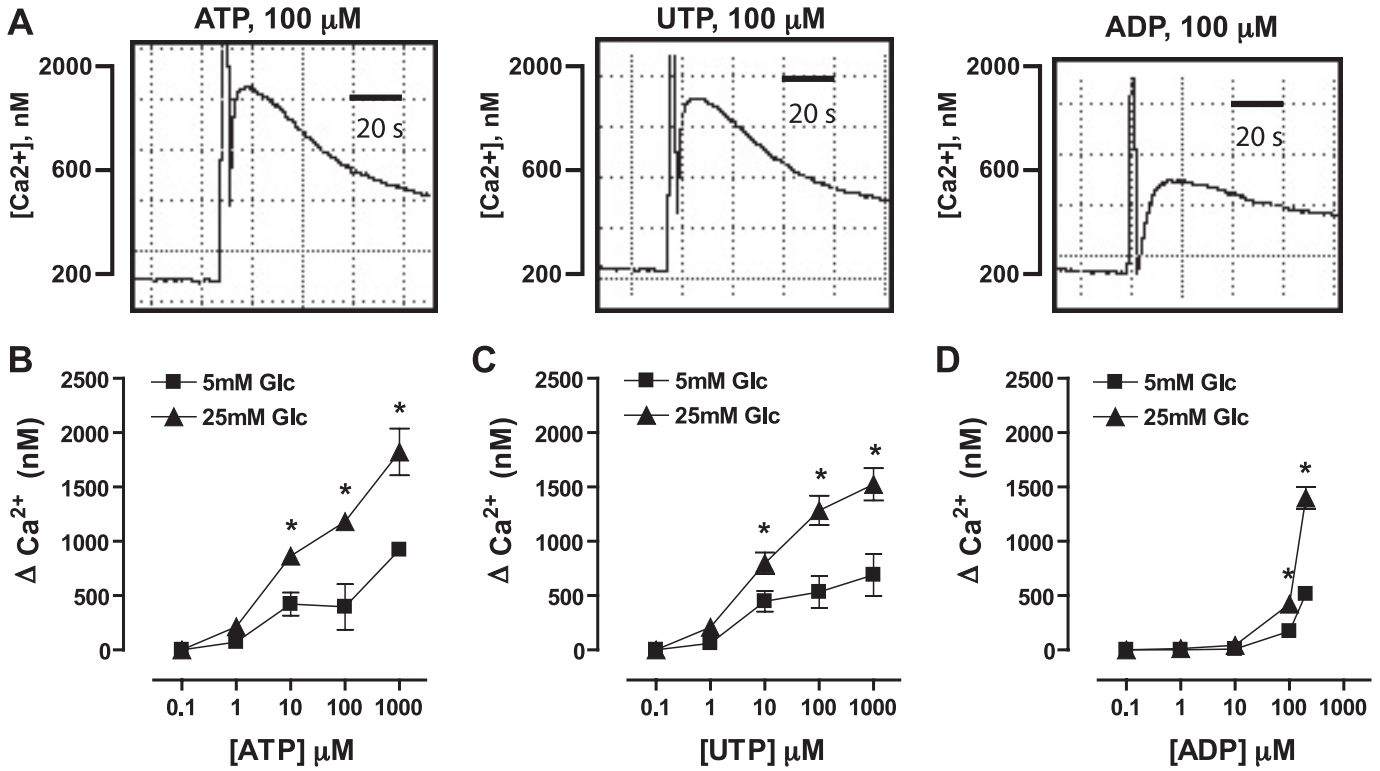

Fig. 6. rMC-1 cells express Gq-coupled, Ca^{2+}-mobilizing P2Y2/P2Y4 and P2Y1 receptors and high-glucose treatment increases the efficacy of Ca^{2+} mobilization. rMC-1 cells were incubated in control medium or high-glucose medium for 24 h and then trypsinized to generate single cell suspensions for fura2 loading and fluorimetric analysis of cytosolic [Ca^{2+}] as described in METHODS (*A–D*). *A*: representative time courses of Ca^{2+} mobilization triggered by 100 mM pulses of ATP, UTP, or ADP. *B–D*: concentration-response relationships describing peak changes in cytosolic Ca^{2+} elicited by the indicated [ATP], [UTP], or [ADP] in rMC-1 cells isolated from the control (■) versus high glucose (▲) culture conditions. Data are the means ± SE ($n = 5$). *$P < 0.05$ compared with control incubated cells (Student's *t*-test).

ing macrophages and microglia, constitutively express high levels of caspase-1 mRNA and protein in its zymogenic procaspase-1 form (4, 27, 39). Accumulation of active caspase-1 at functionally significant levels in myeloid leukocytes is not limited by the amount of procaspase-1 protein but by the levels of key inflammasome adapter proteins, such as NLRP3, and/or the PAMP and DAMP ligands which allosterically regulate assembly of the inflammasome platforms (4, 21, 27, 39). In contrast, procaspase-1 is expressed at lower limiting levels within nonhematopoietic cells, such as pancreatic β cells (39, 59), adipocytes (23, 42), keratinocytes (58), and osteoblasts (3), known to secrete IL-1β in response to sterile proinflammatory stimuli.

Recent studies have indicated upregulation of caspase-1 gene expression per se as a critical component of the inflammasome activation response in such cells. Fibroblastoid cells from the bone tumors of patients with neonatal-onset multisystem inflammatory disease (NOMID) exhibit hyperexpression of caspase-1 due to a cAMP/PKA-driven increase in the Ets-1 transcription factor, which positively modulates caspase-1 gene expression (3). The same study reported that FSK or prostaglandin E2 increased caspase-1 gene expression in MC3T3-E1 murine pro-osteoblasts similar to our findings with rMC-1 glial cells. Undifferentiated 3T3-L1 preadipocytes lack basal expression of caspase-1 but accumulate caspase-1 mRNA and protein during induction of adipocyte differentiation (42). Notably, the classic 3T3-L1 "differentiation cocktail" includes isobutyl-methyl-xanthine, which increases cAMP via inhibition of cAMP-phosphodiesterases. Thus cAMP-dependent regulation of caspase-1 expression to nonlimiting levels may be a general pathway for inflammasome regulation and production of bioactive IL-1β by nonmyeloid cell types exposed to diverse metabolic stress signals.

Most of the stimuli (high glucose, NECA, ATP) that increased caspase-1 activity in rMC-1 cells also upregulated expression of TXNIP but to different levels (Fig. 5*B*). Defining how TXNIP is involved in inflammasome regulation and IL-1β secretion has been an active but contentious area of recent investigation. Zhou et al. (59) reported that TXNIP binds to NLRP3 and is critical for activation of the NLRP3/caspase-1 inflammasome in human THP1 monocytes, primary murine macrophages, and murine pancreatic β cells. That study proposed that increased reactive oxygen species (ROS) production after mitochondrial damage leads to dissociation of TXNIP/thioredoxin complexes, thus freeing thioredoxin to scavenge ROS and TXNIP to interact with NLRP3 and drive inflammasome activation. However, another report that compared P2X7R-dependent or NLRP3-inflammasome activation in macrophages from wild-type versus TXNIP-knockout mice failed to demonstrate a critical role for TXNIP (28). Conversely, analysis of hyperglycemia-induced IL-1β secretion by human adipocytes confirmed a stimulatory role for TXNIP in mature IL-1β production but at the level of increased IL-1β gene expression rather than caspase-1 activation (23, 42). Thus the precise role of TXNIP in caspase-1/IL-1β cascades may

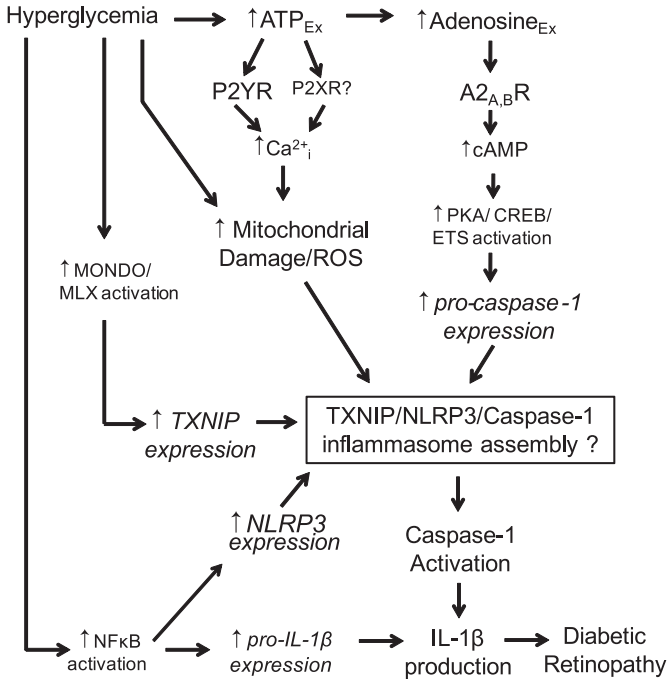

Fig. 7. Proposed model for high-glucose-induced caspase-1 activation via purinergic signaling. See text for definitions of abbreviations.

vary with cell type and/or the relative expression levels of TXNIP and other inflammasome components. It is relevant to note that elevated expression of TXNIP in rat models of retinal inflammation is associated with increased neurotoxicity, endothelial dysfunction, glial activation, and enhanced release of IL-1β and tumor necrosis factor-α. Moreover, knockdown of TXNIP in a rat model of diabetic retinopathy protected against capillary dropout and retinal gliosis, though this effect was not specifically linked to protection of Müller cells from high-glucose stress (2, 34).

Regardless of the precise role(s) for TXNIP in regulating caspase-1 and other high-glucose-induced inflammatory responses in Müller cells, our observations confirm and extend reports regarding the ability of extracellular adenosine and other purines to positively modulate TXNIP gene expression under control and hyperglycemic conditions (56). TXNIP expression is stringently linked to extracellular glucose concentration via glycolytic flux-induced activation of the MondoA and Max-like protein X (MLX) transcription factors that interact with a carbohydrate response element in the TXNIP gene promoter (8, 55, 56). However, incubation of a broad range of cell types with extracellular adenosine or other adenosine-containing compounds, including ATP, also increased transcription of TXNIP by facilitating nuclear translocation of Mondo A (56). Additionally, increased cAMP can decrease TXNIP protein stability (46). High glucose also activates nuclear factor κB (NFκB)-based gene expression in rMC-1 cells (22, 38), and NLRP3 expression in myeloid cells is markedly upregulated by stimuli coupled to NFκB (4, 21). Thus Müller cells exposed to high glucose may coordinately upregulate NLRP3 via NFκB transcriptional signaling, TXNIP via MondoA/MLX transcriptional signaling, and caspase-1 via PKA/CREB/Ets-1 transcriptional signaling (Fig. 7).

Although ADA significantly reduced high-glucose-induced caspase-1 activation to implicate a specific role for adenosine in this regulatory process, treatment with apyrase similarly reduced caspase-1 activation (Fig. 1*A*). These data indicated that ATP per se, and not merely its metabolite adenosine, also participates in regulating caspase-1 activation (Fig. 7). Surprisingly, our experiments demonstrated no significant expression of functional P2X7R in rMC-1 cells or contribution of P2X7R signaling to high-glucose-induced caspase-1 activation (Fig. 4). We explored whether P2X4R, another P2XR subtype recently linked to caspase-1 activation (12, 40), might be involved by testing if ivermectin, which allosterically potentiates ATP-gating of P2X4 channels, would increase ATP-induced Ca^{2+} influx in control or high-glucose-treated rMC-1 cells. However, these experiments failed to identify P2X4-like function in this cell model (data not shown). Rather, several lines of experimental evidence (Figs. 3*A*, 4*A*, 6*B*, and 6*C*) suggested that Gq-coupled, Ca^{2+}-mobilizing P2Y2 receptors may mediate the stimulatory action of exogenous ATP. How ATP, presumably acting via P2Y2R, might increase caspase-1 expression (Fig. 5*B*) and activity (Fig. 2, *A* and *B*) remains to be defined. Plausible mechanisms include Ca^{2+}-dependent induction of mitochondrial ROS implicated in NLRP3- and TXNIP-dependent regulation of inflammasome assembly (Fig. 7). Additionally, activation of P2Y receptors has been shown to regulate osmotic changes within the diseased and damaged retina and may be linked to fluxes of Ca^{2+} or other ions that modulate caspase activity (6, 14, 24, 48, 50). However, exogenous UTP, which also triggered robust Ca^{2+} mobilization (Fig. 6*B*), failed to mimic the ability of exogenous ATP to significantly increase caspase-1 activity (Fig. 2*A*). This could reflect the inability of UTP to additionally support generation of adenosine and activation of A2 receptor signaling. We tested whether combined treatment with UTP, as a nonadenine nucleotide agonist of P2Y2 receptors, plus NECA, as a pan-P1 receptor agonist, would produce additive increases in caspase-1 activation. However, these experiments did not demonstrate any significant differences between treatments with NECA alone or NECA plus UTP (data not shown).

Finally, we noted that exogenous UTP and ADP, in contrast to ATP, attenuated high-glucose activation of caspase-1 (Fig. 2*A*) even when added at submillimolar levels (data not shown). This suggests an additional inhibitory role of P2Y family receptors in the complex multicomponent signaling network that links high-glucose stress to activation of the caspase-1/IL-1β response in Müller cells. Activation of G_i-coupled P2Y receptors that counteract Gs-coupled A2 receptors or drive activation of cAMP phosphodiesterases are possible pathways that should be considered.

In summary, we demonstrate convergence of multiple signaling pathways in a tissue culture model of retinal Müller cells whereby high-glucose conditions regulate caspase-1 activity via a purinergic-dependent but P2X7R-independent mechanism (Fig. 7). Whether similar purinergic cascades regulate caspase-1 in Müller cells within the complex in vivo environment of the intact retina remains an important question for future experiments. If so, inhibition of the relevant adenosine or ATP receptors may protect retinal Müller cells from hyperglycemia-induced inflammation and thereby attenuate the progression of diabetic retinopathy.

ACKNOWLEDGMENTS

We are grateful to Vijay Sarthy for generously providing the rMC-1 cell line.

GRANTS

This research was supported by National Institutes of Health Grants R01-EY017206 (to S. Mohr) and R01-GM36387 (to G. R. Dubyak). K. E. Trueblood was supported by the Visual Sciences Training Grant T32-EY07157 to Case Western Reserve University.

DISCLOSURES

No conflicts of interest, financial or otherwise, are declared by the author(s).

REFERENCES

1. **Adinolfi E, Cirillo M, Woltersdorf R, Falzoni S, Chiozzi P, Pellegatti P, Callegari MG, Pellegatti P, Sandona D, Markwardt F, Schmalzing G, Di Virgilio F.** Trophic activity of a naturally occurring truncated isoform of the P2X7 receptor. *FASEB J* 24: 3393–3404, 2010.
2. **Al-Gayyar MM, Abdelsaid MA, Matragoon S, Pillai BA, El-Remessy AB.** Thioredoxin interacting protein is a novel mediator of retinal inflammation and neurotoxicity. *Br J Pharmacol* 164: 170–180, 2011.
3. **Almeida MQ, Tsang KM, Cheadle C, Watkins T, Grivel JC, Nesterova M, Goldbach-Mansky R, Stratakis CA.** Protein kinase A regulates caspase-1 via Ets-1 in bone stromal cell-derived lesions: a link between cyclic AMP and pro-inflammatory pathways in osteoblast progenitors. *Hum Mol Genet* 20: 165–175, 2011.
4. **Bauernfeind FG, Horvath G, Stutz A, Alnemri ES, MacDonald K, Speert D, Fernandes-Alnemri T, Wu J, Monks BG, Fitzgerald KA, Hornung V, Latz E.** Cutting edge: NF-kappaB activating pattern recognition and cytokine receptors license NLRP3 inflammasome activation by regulating NLRP3 expression. *J Immunol* 183: 787–791, 2009.
5. **Bringmann A, Pannicke T, Grosche J, Francke M, Wiedemann P, Skatchkov SN, Osborne NN, Reichenbach A.** Muller cells in the healthy and diseased retina. *Prog Retin Eye Res* 25: 397–424, 2006.
6. **Ceruti S, Fumagalli M, Villa G, Verderio C, Abbracchio MP.** Purinoceptor-mediated calcium signaling in primary neuron-glia trigeminal cultures. *Cell Calcium* 43: 576–590, 2008.
7. **Chen GY, Nunez G.** Sterile inflammation: sensing and reacting to damage. *Nat Rev Immunol* 10: 826–837, 2011.
8. **Chen JL, Merl D, Peterson CW, Wu J, Liu PY, Yin H, Muoio DM, Ayer DE, West M, Chi JT.** Lactic acidosis triggers starvation response with paradoxical induction of TXNIP through MondoA. *PLoS Genet* 6, 2011.
9. **Coddou C, Yan Z, Obsil T, Huidobro-Toro JP, Stojilkovic SS.** Activation and regulation of purinergic P2X receptor channels. *Pharmacol Rev* 63: 641–683, 2011.
10. **Corriden R, Insel PA.** Basal release of ATP: an autocrine-paracrine mechanism for cell regulation. *Sci Signal* 3: re1, 2010.
11. **Demircan N, Safran BG, Soylu M, Ozcan AA, Sizmaz S.** Determination of vitreous interleukin-1 (IL-1) and tumour necrosis factor (TNF) levels in proliferative diabetic retinopathy. *Eye* 20: 1366–1369, 2006.
12. **Dubyak GR.** Go it alone no more–P2X7 joins the society of heteromeric ATP-gated receptor channels. *Mol Pharmacol* 72: 1402–1405, 2007.
13. **Ferrari D, Pizzirani C, Adinolfi E, Lemoli RM, Curti A, Idzko M, Panther E, Di Virgilio F.** The P2X7 receptor: a key player in IL-1 processing and release. *J Immunol* 176: 3877–3883, 2006.
14. **Francke M, Uhlmann S, Pannicke T, Goczalik I, Uckermann O, Weick M, Hartig W, Wiedemann P, Reichenbach A, Bringmann A.** Experimental dispase-induced retinopathy causes up-regulation of P2Y receptor-mediated calcium responses in Muller glial cells. *Ophthalmic Res* 35: 30–41, 2003.
15. **Frank RN.** Diabetic retinopathy. *N Engl J Med* 350: 48–58, 2004.
16. **Fredholm BB, AP Ij, Jacobson KA, Linden J, Muller CE.** International Union of Basic and Clinical Pharmacology. *LXXXI*. Nomenclature and classification of adenosine receptors–an update. *Pharmacol Rev* 63: 1–34, 2011.
17. **Hamada Y, Fukagawa M.** A possible role of thioredoxin interacting protein in the pathogenesis of streptozotocin-induced diabetic nephropathy. *Kobe J Med Sci* 53: 53–61, 2007.
18. **Hong S, Schwarz N, Brass A, Seman M, Haag F, Koch-Nolte F, Schilling WP, Dubyak GR.** Differential regulation of P2X7 receptor activation by extracellular nicotinamide adenine dinucleotide and ecto-ADP-ribosyltransferases in murine macrophages and T cells. *J Immunol* 183: 578–592, 2009.
19. **Junger WG.** Immune cell regulation by autocrine purinergic signalling. *Nat Rev Immunol* 11: 201–212, 2011.
20. **Kahlenberg JM, Dubyak GR.** Mechanisms of caspase-1 activation by P2X7 receptor-mediated K^+ release. *Am J Physiol Cell Physiol* 286: C1100–C1108, 2004.
21. **Kahlenberg JM, Lundberg KC, Kertesy SB, Qu Y, Dubyak GR.** Potentiation of caspase-1 activation by the P2X7 receptor is dependent on TLR signals and requires NF-kappaB-driven protein synthesis. *J Immunol* 175: 7611–7622, 2005.
22. **Kern TS.** Contributions of inflammatory processes to the development of the early stages of diabetic retinopathy. *Exp Diabetes Res* 2007: 95103, 2007.
23. **Koenen TB, Stienstra R, van Tits LJ, de Graaf J, Stalenhoef AF, Joosten LA, Tack CJ, Netea MG.** Hyperglycemia activates caspase-1 and TXNIP-mediated IL-1beta transcription in human adipose tissue. *Diabetes* 60: 517–524, 2011.
24. **Krugel K, Wurm A, Pannicke T, Hollborn M, Karl A, Wiedemann P, Reichenbach A, Kohen L, Bringmann A.** Involvement of oxidative stress and mitochondrial dysfunction in the osmotic swelling of retinal glial cells from diabetic rats. *Exp Eye Res* 92: 87–93, 2011.
25. **Kusner LL, Sarthy VP, Mohr S.** Nuclear translocation of glyceraldehyde-3-phosphate dehydrogenase: a role in high glucose-induced apoptosis in retinal Muller cells. *Invest Ophthalmol Vis Sci* 45: 1553–1561, 2004.
26. **Li Q, Puro DG.** Diabetes-induced dysfunction of the glutamate transporter in retinal Muller cells. *Invest Ophthalmol Vis Sci* 43: 3109–3116, 2002.
27. **Mariathasan S, Weiss DS, Newton K, McBride J, O'Rourke K, Roose-Girma M, Lee WP, Weinrauch Y, Monack DM, Dixit VM.** Cryopyrin activates the inflammasome in response to toxins and ATP. *Nature* 440: 228–232, 2006.
28. **Masters SL, Dunne A, Subramanian SL, Hull RL, Tannahill GM, Sharp FA, Becker C, Franchi L, Yoshihara E, Chen Z, Mullooly N, Mielke LA, Harris J, Coll RC, Mills KH, Mok KH, Newsholme P, Nunez G, Yodoi J, Kahn SE, Lavelle EC, O'Neill LA.** Activation of the NLRP3 inflammasome by islet amyloid polypeptide provides a mechanism for enhanced IL-1beta in type 2 diabetes. *Nat Immunol* 11: 897–904, 2011.
29. **McDermott MF, Tschopp J.** From inflammasomes to fevers, crystals and hypertension: how basic research explains inflammatory diseases. *Trends Mol Med* 13: 381–388, 2007.
30. **Mohr S, Trueblood, K, Vincent, JA.** High glucose-induced caspase-1 activation in retinal müller cells is bi-phasic involving receptor interacting protein 2 (RIP 2) upregulation. In: *American Diabetes Association 67th Scientific Sessions*. Chicago, IL: Am. Diabetes Assoc., 2007.
31. **Mohr S, Xi X, Tang J, Kern TS.** Caspase activation in retinas of diabetic and galactosemic mice and diabetic patients. *Diabetes* 51: 1172–1179, 2002.
32. **Pannicke T, Fischer W, Biedermann B, Schadlich H, Grosche J, Faude F, Wiedemann P, Allgaier C, Illes P, Burnstock G, Reichenbach A.** P2X7 receptors in Muller glial cells from the human retina. *J Neurosci* 20: 5965–5972, 2000.
33. **Perrone L, Devi TS, Hosoya K, Terasaki T, Singh LP.** Thioredoxin interacting protein (TXNIP) induces inflammation through chromatin modification in retinal capillary endothelial cells under diabetic conditions. *J Cell Physiol* 221: 262–272, 2009.
34. **Perrone L, Devi TS, Hosoya KI, Terasaki T, Singh LP.** Inhibition of TXNIP expression in vivo blocks early pathologies of diabetic retinopathy. *Cell Death Dis* 1: e65, 2011.
35. **Pickup JC.** Inflammation and activated innate immunity in the pathogenesis of type 2 diabetes. *Diabetes Care* 27: 813–823, 2004.
36. **Prosdocimo DA, Douglas DC, Romani AM, O'Neill WC, Dubyak GR.** Autocrine ATP release coupled to extracellular pyrophosphate accumulation in vascular smooth muscle cells. *Am J Physiol Cell Physiol* 296: C828–C839, 2009.
37. **Rock KL, Latz E, Ontiveros F, Kono H.** The sterile inflammatory response. *Annu Rev Immunol* 28: 321–342, 2010.
38. **Romeo G, Liu WH, Asnaghi V, Kern TS, Lorenzi M.** Activation of nuclear factor-kappaB induced by diabetes and high glucose regulates a proapoptotic program in retinal pericytes. *Diabetes* 51: 2241–2248, 2002.
39. **Schroder K, Zhou R, Tschopp J.** The NLRP3 inflammasome: a sensor for metabolic danger? *Science* 327: 296–300, 2010.

40. **Seil M, El Ouaaliti M, Fontanils U, Etxebarria IG, Pochet S, Dal Moro G, Marino A, Dehaye JP.** Ivermectin-dependent release of IL-1beta in response to ATP by peritoneal macrophages from P2X(7)-KO mice. *Purinergic Signal* 6: 405–416, 2010.
41. **Solini A, Chiozzi P, Morelli A, Adinolfi E, Rizzo R, Baricordi OR, Di Virgilio F.** Enhanced P2X7 activity in human fibroblasts from diabetic patients: a possible pathogenetic mechanism for vascular damage in diabetes. *Arterioscler Thromb Vasc Biol* 24: 1240–1245, 2004.
42. **Stienstra R, Joosten LA, Koenen T, van Tits B, van Diepen JA, van den Berg SA, Rensen PC, Voshol PJ, Fantuzzi G, Hijmans A, Kersten S, Muller M, van den Berg WB, van Rooijen N, Wabitsch M, Kullberg BJ, van der Meer JW, Kanneganti T, Tack CJ, Netea MG.** The inflammasome-mediated caspase-1 activation controls adipocyte differentiation and insulin sensitivity. *Cell Metab* 12: 593–605, 2010.
43. **Vandanmagsar B, Youm YH, Ravussin A, Galgani JE, Stadler K, Mynatt RL, Ravussin E, Stephens JM,Dixit VD.** The NLRP3 inflammasome instigates obesity-induced inflammation and insulin resistance. *Nat Med* 17: 179–188, 2011.
44. **Vincent JA, Mohr S.** Inhibition of caspase-1/interleukin-1beta signaling prevents degeneration of retinal capillaries in diabetes and galactosemia. *Diabetes* 56: 224–230, 2007.
45. **von Kugelgen I.** Pharmacological profiles of cloned mammalian P2Y-receptor subtypes. *Pharmacol Ther* 110: 415–432, 2006.
46. **Wang X, Wang H, Figueroa BE, Zhang WH, Huo C, Guan Y, Zhang Y, Bruey JM, Reed JC, Friedlander RM.** Dysregulation of receptor interacting protein-2 and caspase recruitment domain only protein mediates aberrant caspase-1 activation in Huntington's disease. *J Neurosci* 25: 11645–11654, 2005.
47. **Ward MM, Jobling AI, Kalloniatis M, Fletcher EL.** Glutamate uptake in retinal glial cells during diabetes. *Diabetologia* 48: 351–360, 2005.
48. **Wurm A, Erdmann I, Bringmann A, Reichenbach A, Pannicke T.** Expression and function of P2Y receptors on Muller cells of the postnatal rat retina. *Glia* 57: 1680–1690, 2009.
49. **Wurm A, Lipp S, Pannicke T, Linnertz R, Farber K, Wiedemann P, Reichenbach A, Bringmann A.** Involvement of A(1) adenosine receptors in osmotic volume regulation of retinal glial cells in mice. *Mol Vis* 15: 1858–1867, 2009.
50. **Wurm A, Lipp S, Pannicke T, Linnertz R, Krugel U, Schulz A, Farber K, Zahn D, Grosse J, Wiedemann P, Chen J, Schoneberg T, Illes P, Reichenbach A, Bringmann A.** Endogenous purinergic signaling is required for osmotic volume regulation of retinal glial cells. *J Neurochem* 112: 1261–1272, 2011.
51. **Wurm A, Pannicke T, Iandiev I, Francke M, Hollborn M, Wiedemann P, Reichenbach A, Osborne NN, Bringmann A.** Purinergic signaling involved in Muller cell function in the mammalian retina. *Prog Retin Eye Res* 2011, ePub ahead of print.
52. **Xi X, Gao L, Hatala DA, Smith DG, Codispoti MC, Gong B, Kern TS, Zhang JZ.** Chronically elevated glucose-induced apoptosis is mediated by inactivation of Akt in cultured Muller cells. *Biochem Biophys Res Commun* 326: 548–553, 2005.
53. **Yego EC, Mohr S.** siah-1 Protein is necessary for high glucose-induced glyceraldehyde-3-phosphate dehydrogenase nuclear accumulation and cell death in Muller cells. *J Biol Chem* 285: 3181–3190, 2011.
54. **Yego EC, Vincent JA, Sarthy V, Busik JV, Mohr S.** Differential regulation of high glucose-induced glyceraldehyde-3-phosphate dehydrogenase nuclear accumulation in Muller cells by IL-1beta and IL-6. *Invest Ophthalmol Vis Sci* 50: 1920–1928, 2009.
55. **Yu FX, Chai TF, He H, Hagen T, Luo Y.** Thioredoxin-interacting protein (Txnip) gene expression: sensing oxidative phosphorylation status and glycolytic rate. *J Biol Chem* 285: 25822–25830, 2010.
56. **Yu FX, Goh SR, Dai RP, Luo Y.** Adenosine-containing molecules amplify glucose signaling and enhance txnip expression. *Mol Endocrinol* 23: 932–942, 2009.
57. **Yuan J, Lipinski M, Degterev A.** Diversity in the mechanisms of neuronal cell death. *Neuron* 40: 401–413, 2003.
58. **Zepter K, Haffner A, Soohoo LF, De Luca D, Tang HP, Fisher P, Chavinson J, Elmets CA.** Induction of biologically active IL-1 beta-converting enzyme and mature IL-1 beta in human keratinocytes by inflammatory and immunologic stimuli. *J Immunol* 159: 6203–6208, 1997.
59. **Zhou R, Tardivel A, Thorens B, Choi I, Tschopp J.** Thioredoxin-interacting protein links oxidative stress to inflammasome activation. *Nat Immunol* 11: 136–140, 2010.
60. **Zipfel GJ, Babcock DJ, Lee JM, Choi DW.** Neuronal apoptosis after CNS injury: the roles of glutamate and calcium. *J Neurotrauma* 17: 857–869, 2000.